PARAMETERIZATION OF MOIST CONVECTIVE EFFECTS ON THE THERMODYNAMIC AND MOISTURE FIELDS IN NUMERICAL MODELS[1]

R.A. Anthes
National Center for Atmospheric Research[2]
Boulder, Colorado, U.S.A.

1. INTRODUCTION

Because deep cumulus convection is associated with strong diabatic heating rates (up to 500 K/day in an intense thunderstorm) and are vigorous transporters of heat and water from the lower to the upper troposphere, they have a significant effect on the larger scale (mesoscale and synoptic scale) temperature and moisture fields, and this effect must be parameterized in realistic atmospheric models of the mesoscale and the global scale.

The problem of cumulus parameterization is to relate the convective condensation and transports of heat, moisture, and momentum by cumulus clouds, which cannot be explicitly resolved by the large-scale model, to the variables predicted by the model. There are two important aspects of cumulus parameterization. One is the modulation of convection by the large-scale forcing, which is related to the determination of total rainfall rate. The other is the feedback of cumulus convection to its environment, which is related to the vertical distribution of condensation and evaporation in the clouds and the vertical transports of heat,

---

[1]Paper presented at the 1985 ECMWF Seminar "Physical Parameterizations for Numerical Models," Shinfield Park, Reading, United Kingdom, 9-13 September 1985.

[2]The National Center for Atmospheric Research is sponsored by the National Science Foundation.

moisture, and momentum. For parameterization to be possible, a relationship between cumulus convection and the large-scale circulation must exist. Since the scales of motion permitted in the model depend on the grid size, one might expect the relationships between the resolvable-scale and the unresolvable-scale circulations to vary with different model resolutions.

Several cumulus parameterization schemes have been used in numerical models of large-scale phenomena. These schemes are (1) moist convective adjustment schemes, (2) Kuo schemes, (3) the Arakawa and Schubert (1974) scheme, and (4) schemes based on local consumption of available buoyant energy (Kreitzberg and Perkey, 1976; Fritsch and Chappell, 1980). A detailed review of all four types is beyond the scope of this paper, and brief summaries exist elsewhere (Frank, 1983). Therefore, this paper discusses only the first two types of schemes.

2. MOIST CONVECTIVE ADJUSTMENT

Moist convective adjustment (MCA) schemes are among the simplest methods of parameterizing the effects of cumulus convection on the environment. In MCA parameterizations, it is assumed that there exists a critical temperature and moisture profile associated with the large-scale thermodynamic field. When the large-scale sounding becomes more unstable than this critical state, it is adjusted toward the critical, more stable state. This stabilization is assumed to be caused by cumulus convection.

A variety of MCA schemes has been proposed and tested in models (Manabe et al., 1965; Miyakoda et al., 1969; Krishnamurti and Moxim, 1971; Kurihara, 1973). In its most severe form, the so-called hard convective

adjustment, an initial large-scale sounding in which $\partial\theta_e/\partial p > 0$ is adjusted so that θ_e or, equivalently, moist static energy h, is constant with height (Krishnamurti et al., 1980). The precipitation rate P is determined from the adjusted sounding according to

$$P = \frac{1}{g\Delta\tau} \int_{p_t}^{p_s} (q^i - q^f)\, dp \,, \tag{1}$$

where $\Delta\tau$ is a prescribed time scale associated with the lifetime of a deep cumulus cloud (~30 min), and i and f denote initial and adjusted values of q, respectively.

The hard MCA is simple to implement and conserves total moist static energy, since the average value of h in the adjusted sounding is equal to that of the initial sounding. However, it produces unrealistic modifications to the large-scale sounding by excessively cooling and drying the lower troposphere. Because of the removal of too much water vapor during the adjustment, the rainfall rates diagnosed by (1) are much too large. Krishnamurti et al. (1980) used GATE data over the period 1 September to 18 September 1974 in semi-prognostic tests of the hard MCA scheme. (In a semi-prognostic test, observed estimates of horizontal and vertical advection, surface fluxes, and radiational heating are used to calculate the large-scale forcing terms in a parameterization scheme. The effects of cumulus convection on the environment are calculated from these terms and can then be compared against those diagnosed from large-scale budgets.) The diagnosed rainfall rates from the hard MCA (Fig. 1) exceed the observed rainfall rates by more than an order of magnitude. Because of the unrealistic modification to the large-scale thermodynamic fields and the erroneous rainfall rates, the hard MCA may be considered unsuitable for use in large-scale models.

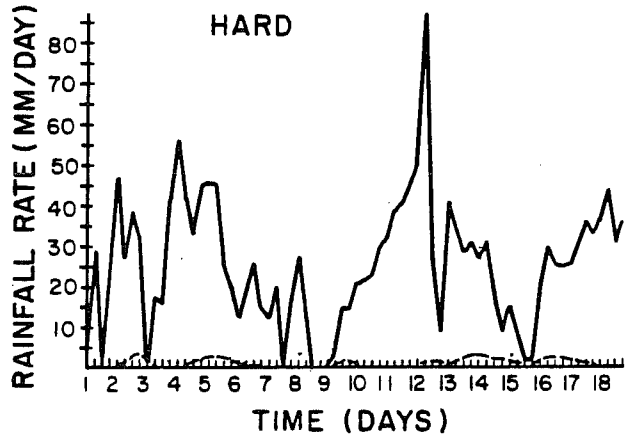

Fig. 1 Comparison of observed (dashed) and predicted (solid) rainfall rates (mm day^{-1}) using hard convective adjustment. Days 1 to 18 correspond to the third phase of GATE between 1 September and 18 September 1974. Data are for 6-h intervals beginning with 0000 GMT 1 September (Krishnamurti et al., 1980).

Because of the problems associated with the hard MCA schemes, several versions of MCA have been developed which produce much slower and more realistic adjustments to the large-scale sounding (Manabe et al., 1965; Miyakoda et al., 1969; Kurihara, 1973; Krishnamurti et al., 1980). These methods are known as soft adjustment schemes. In one of the soft schemes, hard adjustment is assumed to occur over a small fraction a of the large-scale grid area; over the remaining (1 - a) fraction, the temperature and mixing ratio are assumed to remain constant at their initial value. The final adjusted large-scale values of T and q are given by

$$T^f = aT_c + (1 - a)\, T^i \,, \qquad q^f = aq_c + (1 - a)\, q^i \,, \tag{2}$$

where T_c and q_c are determined by a moist adiabat. The value of a is determined by a criterion based on mean relative humidity of the column. The relative humidity after adjustment RH^f is

$$RH^f = \frac{q^f}{q_s(T^f)}, \tag{3}$$

where $q_s(T^f)$ is the saturation mixing ratio at the adjusted temperature. The scheme is closed by an iterative search for a value of a which yields a vertical mean RH^f equal to that of a prescribed value $\overline{RH}$. In semi-prognostic tests of this soft MCA, Krishnamurti et al. (1980) found best agreement between calculated and observed rainfall rates when $\overline{RH}$ = 82.4% (Fig. 2).

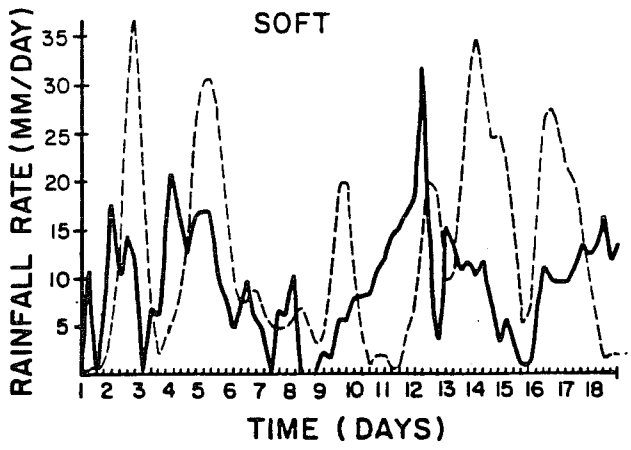

Fig. 2 As in Fig. 1, except for using soft convective adjustment (Krishnamurti et al., 1980).

As shown in Fig. 2, the soft MCA produces rainfall rates of the correct order of magnitude. However, because of the occurrence of the maximum instability before the time of maximum convection in the tropics, the soft MCA scheme shows a lag of one to two days between the computed and observed rainfall. This lag makes the soft MCA scheme undesirable for

use in forecast models in which predicting the correct timing of rainfall is as important as predicting the correct amount. However, the soft MCA may be more suitable for climate models in which the timing of precipitation is less important.

3. KUO SCHEMES

As reviewed by Anthes (1985), there is a strong correlation between observed convective rainfall and total large-scale convergence of water vapor in a column. These observations suggest that large-scale water vapor convergence is a useful variable to parameterize the effects of convection in large-scale models, and many cumulus parameterizations have been based on a relationship between convective rainfall and large-scale moisture convergence. These schemes are called Kuo schemes here because of the early work by Kuo (1965). Versions of the Kuo (1965) scheme include those by Kuo (1974), Anthes (1977), Lian (1979), Krishnamurti et al. (1976, 1980, 1983), and Molinari (1982).

3.1 Relation of total convective heating and moistening to moisture convergence

The use of moisture convergence to determine the rainfall rate is based on the large-scale water vapor budget, which may be written (Anthes, 1985)

$$\frac{c_p}{L} Q_2 = - \left(\frac{\partial q}{\partial t} + \nabla \cdot q\underset{\sim}{V} + \frac{\partial q\omega}{\partial p}\right) = \frac{\overline{\partial q' \omega'}}{\partial p} + (c - e) \ , \qquad (4)$$

where c is the rate of condensation per unit mass of air, and e is the rate of evaporation.

A vertical integration of (4) from the surface pressure p_s to the top of the atmosphere (p = 0) yields

$$M_t + E = \frac{1}{g} \int_0^{p_s} (c - e)\, dp + S_{qv} , \tag{5}$$

where M_t is the vertically integrated horizontal moisture convergence

$$M_t \equiv - \frac{1}{g} \int_0^{p_s} \nabla \cdot q \underset{\sim}{V}\, dp , \tag{6}$$

E is the surface evaporation rate

$$E \equiv - \frac{1}{g} \left(\overline{q'\omega'}\right)_{p_s} , \tag{7}$$

and S_{qv} is the storage rate of water vapor.

$$S_{qv} \equiv \frac{1}{g} \int_0^{p_s} \frac{\partial q}{\partial t}\, dp . \tag{8}$$

The relationship between the integrated net condensation and the precipitation rate can be obtained by considering the equation for cloud (liquid) water q_ℓ

$$\frac{\partial q_\ell}{\partial t} + \nabla \cdot q_\ell \underset{\sim}{V} + \frac{\partial q_\ell \omega}{\partial p} = - \frac{\overline{\partial q_\ell' \omega'}}{\partial p} + c - e - r , \tag{9}$$

where r is the rate of conversion of cloud water to precipitating water. A vertical integration of (9) from 0 to p_s yields

$$\frac{1}{g} \int_0^{p_s} (c - e)\, dp = P + S_{q\ell} - M_{t_\ell} , \tag{10}$$

where P is the precipitation rate, $S_{q\ell}$ is the storage rate of liquid water, and $M_{t\ell}$ is the vertical integral of the horizontal convergence of liquid water.

Substitution of (10) into (5) yields

$$M_t + M_{t_\ell} + E = P + S_{qv} + S_{q\ell} . \qquad (11)$$

The budget represented by (11) indicates that the sources of water into a unit column are balanced by precipitation plus storage of vapor and liquid.

From (11), one observes that if the storage terms are small and the horizontal convergence of liquid water is small compared to the sum of the evaporation and the water vapor convergence, the net rainfall rate is equal to the large-scale moisture convergence plus the evaporation. Over large regions on a long temporal scale, this approximation is quite good. But, locally, on a short temporal scale, there can be substantial changes in the storage of water vapor and liquid water. In general, there is higher variability over midlatitudes than over the tropics. A key issue is then to relate the storage term to the large-scale variables (e.g., to determine what portion of the moisture convergence should go to storage and what portion should be removed as precipitation).

Kuo (1974) assumed that a fraction (1 - b) of the total water vapor convergence M_t is condensed and precipitated, while the remaining fraction b is stored and acts to increase the humidity of the column (Fig. 3).

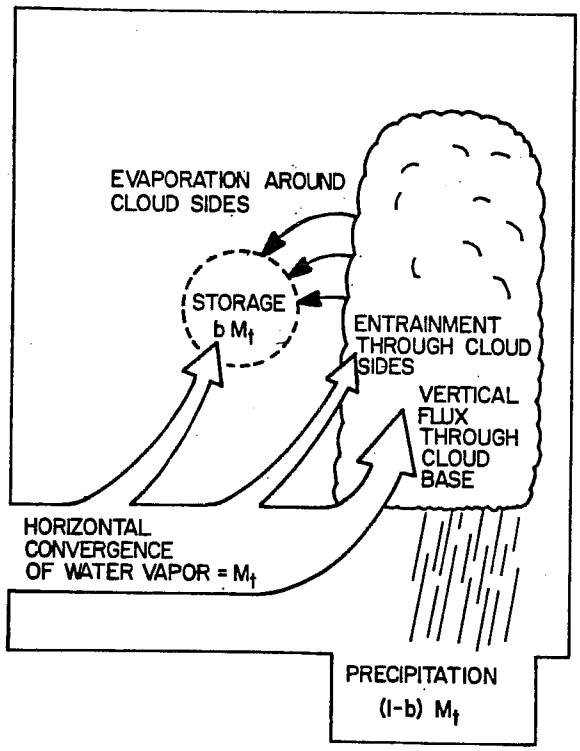

Fig. 3 Schematic diagram showing moisture cycle in a column which contains convection (Anthes, 1977).

By the above assumption, the vertical integral of (c - e) $\equiv$ C* is

$$\int_0^{p_s} C^* dp = (1 - b)\ g\ M_t \ . \qquad (12)$$

The determination of b is discussed in section 3.4.

3.2 Vertical partitioning of apparent heat source

After b is determined, the integral relation (12) relates the total rainfall rate to the total moisture convergence. It is also necessary to specify or calculate the vertical distribution of C*; in general, this distribution may be written

$$C^*(p) = \frac{(1-b)\, gM_t}{(p_b - p_t)} N(p) \ , \tag{13}$$

where p_b and p_t are the pressures at cloud base and cloud top, respectively, and N(p) is the vertical distribution function which obeys

$$\int_0^{p_s} N(p)\ dp = \int_{p_t}^{p_b} N(p)\ dp = p_b - p_t \ . \tag{14}$$

If (14) is satisfied, the total convective heating rate $Q_1 - Q_R$ in the column equals the latent energy condensed and removed as precipitation plus the surface sensible heat flux,

$$\frac{c_p}{g} \int_0^{p_s} (Q_1 - Q_R)\ dp = \frac{L}{g} \int_0^{p_s} C^*\ dp + H_s$$

$$= L(1 - b)\ M_t + H_s \ . \tag{15}$$

With the integral constraints represented by (13)-(15), the remaining problem is to determine N(p). As discussed earlier, this function has the same vertical distribution as does the cloud-scale net condensation. Anthes (1977) used the condensation rate C_c in a one-dimensional cloud model to estimate N(p),

$$N(p) \equiv \frac{C_c}{\langle C_c \rangle} \ , \tag{16}$$

where the vertical averaging operator < > is defined by

$$\langle\ \rangle \equiv (p_b - p_t)^{-1} \int_{p_t}^{p_b} (\ )\ dp \ . \tag{17}$$

Kuo (1965, 1974) assumed that N(p) was determined by lateral mixing of warm cloud air of temperature T_c with environmental air of temperature T, which gives

$$N(p) \equiv \frac{(T_c - T)}{\langle T_c - T \rangle} . \tag{18}$$

In most Kuo schemes, T_c is given by the wet adiabat associated with the equivalent potential temperature of a parcel of air originating near the surface.

Kuo and Anthes (1984b) compared the vertical profiles of convective heating computed from (16) with that given by (18) for an extratropical convective system. The convective system was observed over Oklahoma and Kansas as part of the AVE-SESAME 1979 special experiment. Fig. 4 shows the observed and simulated convective heating profile by the Anthes and Kuo schemes for three different cloud radii without the inclusion of eddy sensible heat flux. The observed Q_1 is an average over an area 550 km by 550 km centered over Oklahoma and over a period of time (1800 GMT 10 April 1979 to 1200 GMT 11 April) when the area-averaged rainfall exceeded 1 mm day^{-1}. When the cloud radius is small (Fig. 4a), the two formula, by coincidence, give nearly identical profiles. Both simulate the maximum heating at a considerably lower level than the observed. As the cloud radius increases, the maxima in the two simulated convective heating profiles shift upward and hence become closer to the observed profile, with the maximum in Kuo's profile slightly higher than that of Anthes's.

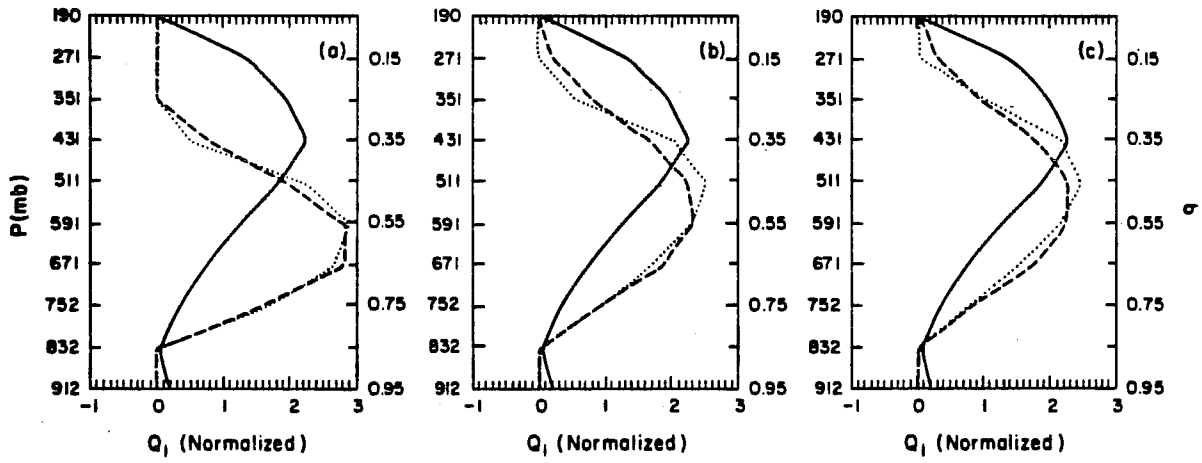

Fig. 4 Observed (solid) and simulated (normalized) Q_1 profiles by cumulus parameterization schemes of Kuo (1974), dotted) and Anthes (1977, dashed), averaged over 550 × 550 km^2 over Oklahoma and for periods of the 10-11 April 1979 case when the observed rainfall rate was greater than 1 mm day^{-1}; (a) for model cloud radii equal to 1 km, (b) 3 km, and (c) 5 km, with no eddy sensible heat flux considered (Kuo and Anthes, 1984b).

We next estimate the heating associated with the vertical divergence of the eddy heat flux associated with convection. In sigma coordinates, the two terms associated with the eddy flux of sensible heat are

$$- \frac{\overline{\partial \dot{\sigma}' T'}}{\partial \sigma} + \frac{\overline{R\ \omega' T'}}{c_p (p^* \sigma + p_t)} \quad . \tag{19}$$

The second term is usually one order of magnitude smaller than the first term and is neglected in the following discussion. For a small fraction of convective cloud cover, a << 1, and with the cloud vertical motion much larger than the large-scale vertical motion, they can be written as

$$\frac{\overline{\partial \dot{\sigma}' T'}}{\partial \sigma} = \frac{\partial}{\partial \sigma} \left[\frac{a}{1 - a} \dot{\sigma}_c (T_c - T) \right] . \tag{20}$$

The fractional area of active convective cloud coverage can be computed as

$$a = \frac{P}{P_c} , \tag{21}$$

where P is the observed area-averaged rainfall rate and P_c is the rainfall rate of a single cloud.

The effect of the eddy sensible heat flux is to shift upward the maximum in the convective heating profiles (Fig. 5). With the increase of cloud radius, the effect of eddy sensible heat flux increases (Fig. 6). The rapid decrease of the cloud vertical motion near the cloud top for large clouds produces a strong eddy flux convergence and hence strong warming below the cloud top. The effect of eddy flux of sensible heat is not negligible compared to the condensation heating for large clouds. With the inclusion of eddy flux of sensible heat and with a large cloud radius, both the Kuo (1974) and Anthes (1977) schemes give a close reproduction of the convective heating profile.

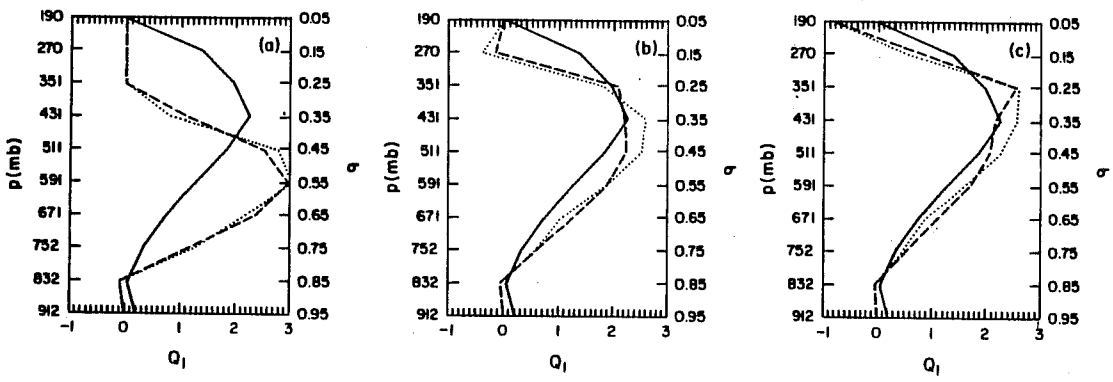

Fig. 5 As in Fig. 4, but with eddy sensible heat flux considered.

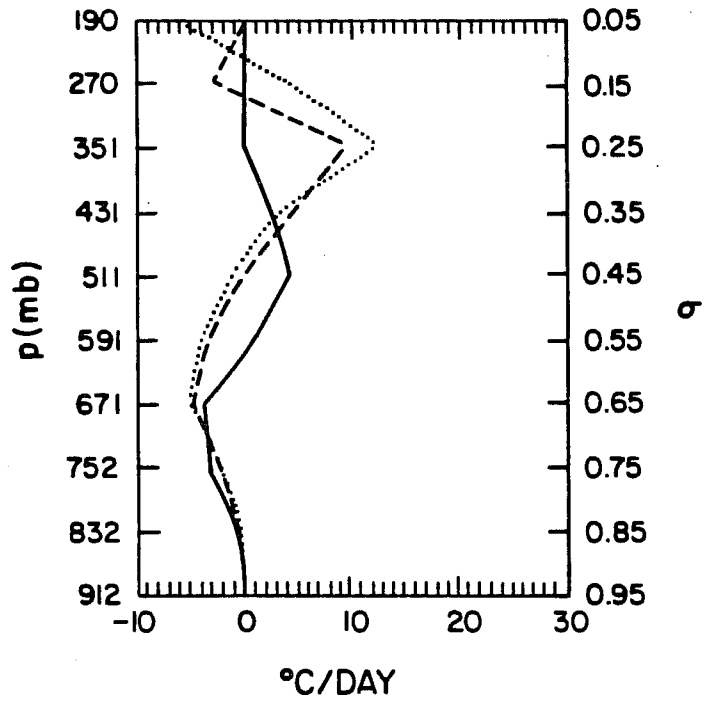

Fig. 6 Eddy sensible heat flux divergence (°C day^{-1}) for clouds with radii of 1 km (solid), 3 km (dashed), and 5 km (dotted) (Kuo and Anthes, 1984b).

To consider an extreme case, the entrainment is set to zero. With no entrainment, a wet adiabat represents the cloud temperature and mixing ratio. The Q_1 profiles (Fig. 7) are very similar to those computed from a large cloud radius with entrainment and are very close to the observed profile. These results suggest that entrainment is not important for strong convection of this type.

The above analysis indicates that both the Kuo (1974) and Anthes (1977) schemes can reproduce the convective heating profile reasonably well when a large cloud radius is used (or when entrainment is suppressed). It also suggests that the effect of eddy flux of sensible heat is quite important in midlatitude convection and should not be ignored in a cumulus parameterization scheme.

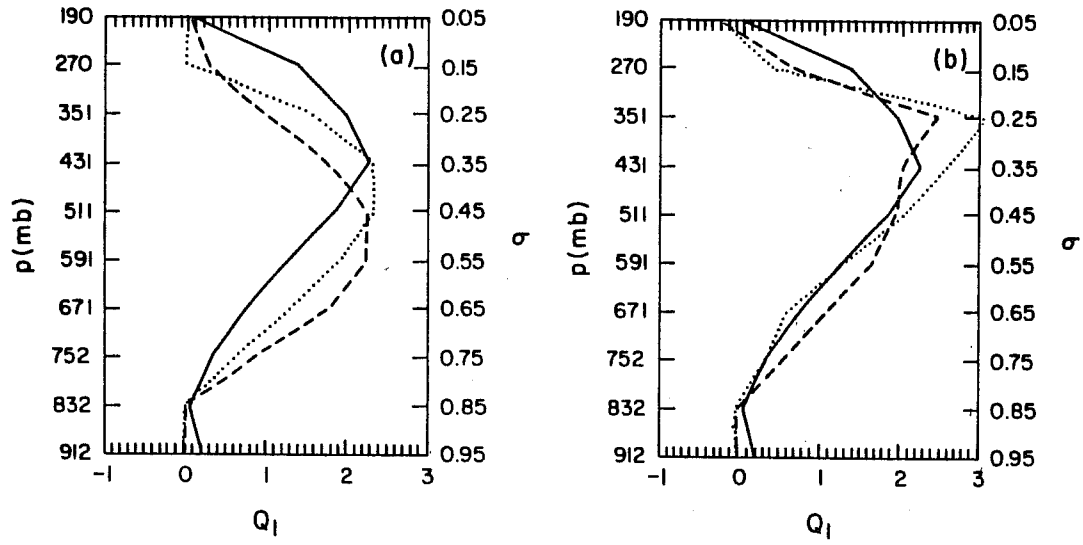

Fig. 7 Observed (solid) and simulated Q_1 profiles (normalized) by cumulus parameterization schemes of Kuo (1974, dotted) and Anthes (1977, dashed), with no entrainment, averaged over 550 km × 550 km box over Oklahoma, and over periods with the observed rainfall rate greater than 1 mm day^{-1}; (a) without eddy sensible heat flux, and (b) with eddy sensible heat flux (Kuo and Anthes, 1984b).

3.3 Vertical partitioning of apparent moisture sink

A fundamental assumption of Kuo schemes is that a fraction b of the total water vapor convergence is used to increase the humidity of the column. Therefore, in columns with convection the continuity equation for water vapor is written

$$\frac{\partial q}{\partial t} = \frac{g\, b\, M_t}{(p_b - p_t)} N_q(p) - \frac{\partial \overline{\omega' q'}}{\partial p} , \tag{22}$$

where $N_q(p)$, the vertical distribution function for water vapor, satisfies an integral constraint like (14). Various empirical functions have been proposed for $N_q(p)$; in the Kuo (1974) scheme,

$$N_q(p) = \frac{q_c - q}{\langle q_c - q \rangle} , \tag{23}$$

where q_c is given by the wet adiabat used to compute T_c in (18). Anthes (1977) suggested that the convective moistening be a function of the relative humidity

$$N_q(p) = \frac{(100\% - RH)\, q_s(T)}{\langle (100\% - RH)\, q_s(T) \rangle} . \tag{24}$$

Eq. (24) was later (Anthes et al., 1982) further simplified to

$$N_q(p) = \frac{q_s}{\langle q_s \rangle} , \tag{25}$$

with the assumption that the relative humidity is fairly uniform in the vertical over areas of strong convection.

For all of these schemes to be valid, it is essential that the vertically integrated moisture convergence is greater than the rainfall rate, so that b is positive. However, observations show that at times the convective precipitation exceeds the total moisture convergence, implying a negative b (Fritsch et al., 1976; Cho, 1976; Kuo and Anthes, 1984a).

One can revise the Kuo schemes by using the complete water vapor continuity equation (4) and utilizing the condensation profile and eddy flux profile predicted by the cloud model. This will also enable the prediction of convective drying (Q_2) profile consistent with that of the convective heating profile (Q_1). With the inclusion of eddy moisture flux, the normalized convective drying profile (Q_2) can be written as

$$N_q(\sigma) = \frac{ac(\sigma) + \overline{\frac{\partial \dot{\sigma}' q'}{\partial \sigma}}}{\left\langle ac(\sigma) + \overline{\frac{\partial \dot{\sigma}' q'}{\partial \sigma}} \right\rangle} . \qquad (26)$$

The cloud coverage, a, can be computed following (21), and the effect of eddy moisture flux can be estimated by an equation analogous to (20).

The observed and simulated normalized Q_2 profiles by the revised scheme averaged over the 550 km x 550 km box and over periods when the rainfall rate is larger than 1 mm day^{-1} (1800 GMT 10 April - 1200 GMT 11 April) are shown in Fig. 8. Most of the observed moisture sink (Q_2) is below 600 mb, while most of the simulated condensation occurs in the middle troposphere. As the cloud radius is increased, the

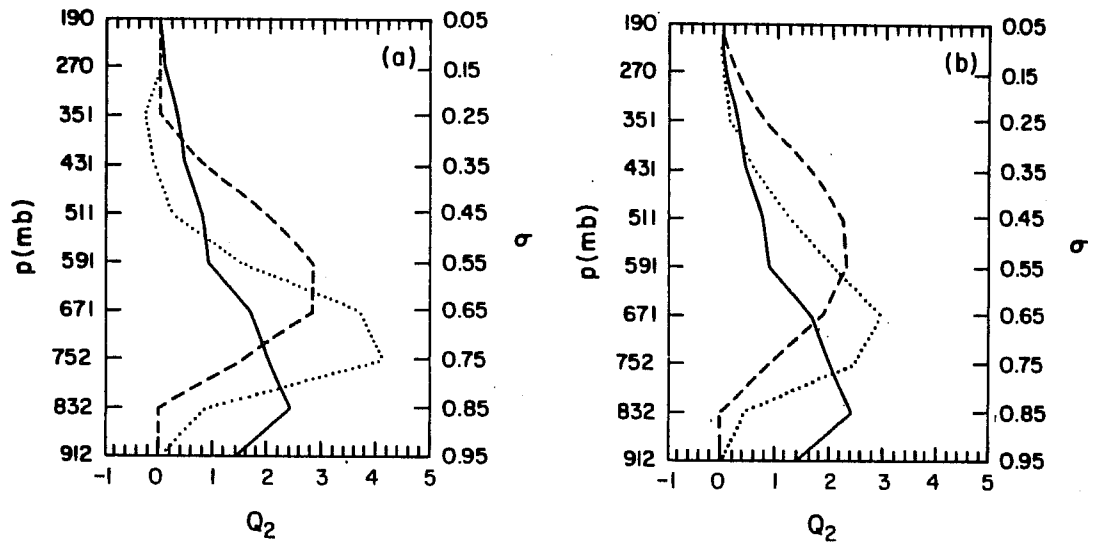

Fig. 8 Observed (solid) and simulated Q_2 profiles (normalized) by revised Anthes scheme with (dotted) and without (dashed) eddy moisture flux averaged over 550 km × 550 km box over Oklahoma and over periods when the observed rainfall rate was greater than 1 mm day^{-1}; (a) 1 km, and (b) 3 km; cloud radius is used in the steady-state cloud model (Kuo and Anthes, 1984b).

simulated condensation profile has its maximum at a slightly higher level. There are larger discrepancies between the simulated and observed Q_2 profiles when eddy moisture flux is ignored. The inclusion of eddy moisture flux shifts the simulated Q_2 profile downward and improves the scheme considerably. Better agreement is found when larger cloud radius is used (Fig. 8) or when entrainment is suppressed (not shown).

The convective eddy flux convergence of latent heat (moisture) is shown in Fig. 9. Its magnitude is compatible with that of the condensation heating. This again supports the importance of eddy flux of moisture by cumulus convection.

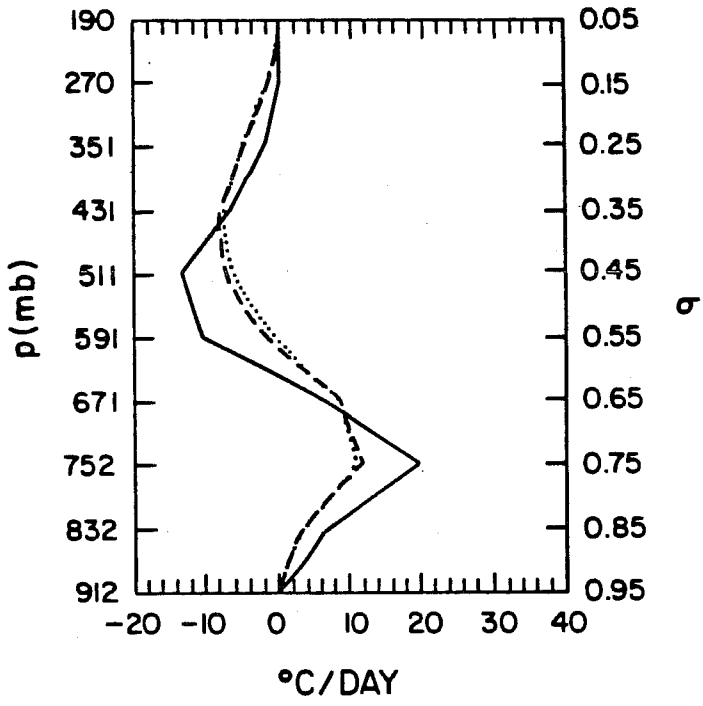

Fig. 9 Eddy latent heat flux convergence estimated by the steady-state cloud model with 1-km radius (solid), 3-km radius (dashed), and 1-km radius without entrainment (dotted), averaged over the same area and period as Fig. 8 (Kuo and Anthes, 1984b).

Despite the improvement made by the inclusion of eddy moisture flux, substantial discrepancies still exist between the observed and simulated Q_2 profiles. The revised scheme overestimates the moisture sink above 800 mb and underestimates the moisture sink below this level. Since the modeled cloud base is at about 830 mb, these discrepancies cannot be eliminated by an increase of cloud radius. It is well-known that shallow nonprecipitating convection can transport substantial moisture from the sub-cloud layer to the cloud layer, so that these differences might have been caused by the neglect of shallow convection in this scheme. The turbulence exchange of moisture between the planetary boundary layer and the free troposphere could also contribute to the large observed moisture sink in the lower layers.

Although the Kuo (1965), Anthes (1977), and Anthes et al. (1982) schemes are not valid after the mature stage of the convective system when the rainfall exceeds the moisture convergence (because b in these schemes cannot be negative), it is of interest to see how these schemes perform during the developing stage of the convective event when the observed b is positive. Fig. 10 shows the normalized observed and simulated convective moistening profiles averaged over the developing period of the convective system (1500 GMT 10 April - 2100 GMT 10 April) over the 550 km × 550 km box.

With the inclusion of eddy moisture flux, the Anthes et al. (1982) scheme shows some differences from the observed profile at small cloud radius (Fig. 10). However, when the cloud radius is increased (or when entrainment is removed), the Anthes et al. (1982) scheme reproduces the general pattern of the convective moistening profile. The inclusion of convective eddy moisture flux does not improve the Kuo (1965) scheme

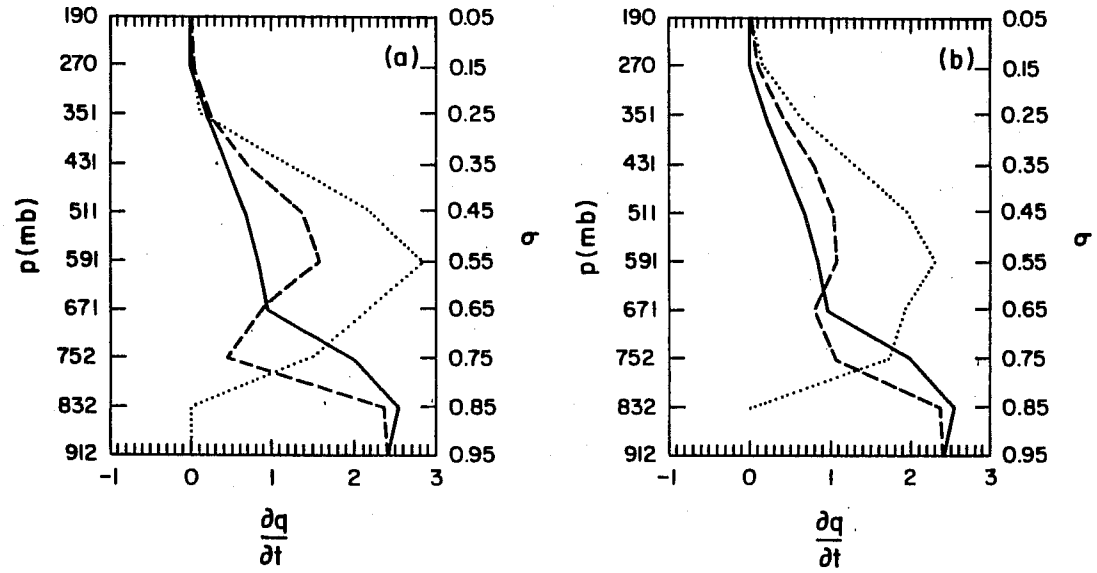

Fig. 10 Observed (solid) and simulated normalized convective moistening ($\partial q/\partial t$) profiles by cumulus parameterization schemes of Kuo (1965, dotted) and Anthes et al. (1982, dashed) averaged over 550 km × 550 km box over Oklahoma and over the developing stage of the extratropical convective system for cloud radii equal to (a) 1 km, and (b) 3 km, with inclusion of eddy moisture flux (Kuo and Anthes, 1984b).

very much. Since most of the convective moistening occurs in the lower troposphere, while (q_c - q) can only exist above the cloud base, these errors cannot be eliminated by either the inclusion of eddy sensible moisture flux or the variation of cloud radius.

The shape of the observed ($\partial q/\partial t$) profile shows that most of the moistening exists in the lower troposphere. Since the moisture content also decreases with height, these results suggest that, during the developing stage, the net effect of the large-scale and convective redistribution of moisture is to increase the environment relative humidity rather uniformly in the vertical.

3.4 Determination of b

An important part of the Kuo schemes is the determination of the parameter b, the fraction of M_t used to moisten the column. Kuo (1965) partitioned the total rate of supply of moisture I into two parts, I_1 and I_2, where I_1 is the portion of I that is condensed and removed as precipitation, thereby increasing the temperature of the cloud column from T to T_c,

$$I_1 \equiv \frac{c_p}{L} \int_{p_t}^{p_b} (T_c - T)\, dp \,, \tag{27}$$

and I_2 is the part of I required to raise the mixing ratio of the cloud column from q to q_c

$$I_2 \equiv \int_{p_t}^{p_b} (q_c - q)\, dp \,. \tag{28}$$

After I is used to create a cloud of temperature T_c and mixing ratio q_c, the large-scale temperature and moisture changes are computed by horizontal mixing of the cloud with its environment, with the total heating proportional to I_1 and the total moistening proportional to I_2. Although Kuo (1965) did not formally define a b parameter, an effective b for the 1965 scheme can be computed from the ratio of I_1 and I_2

$$b \equiv \frac{I_2}{I_1 + I_2} = \frac{\langle q_c - q \rangle}{\left\langle \frac{c_p}{L} (T_c - T) + q_c - q \right\rangle} \,. \tag{29}$$

Kuo (1965) notes that, for a typical tropical sounding, I_1/I_2 is about 0.25, which yields a value of b of about 0.8. Thus, in the original Kuo scheme, most of the available moisture supply was used to

moisten rather than heat the column, with a resulting underprediction of of rainfall (Fig. 11). Observations (Kuo, 1974; Krishnamurti et al., 1980) indicate b to be in the range 0.23-0.26.

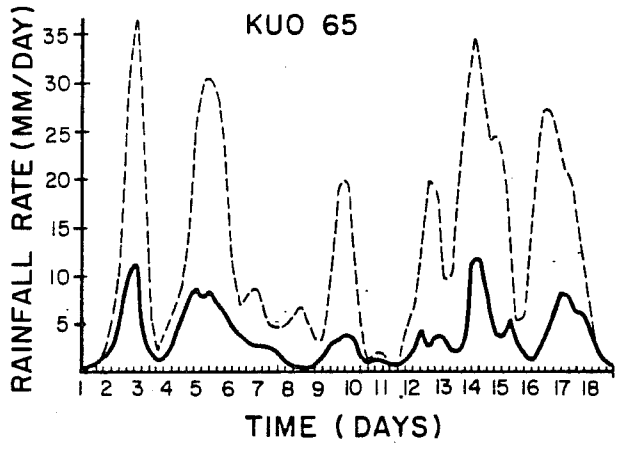

Fig. 11 Comparison between observed (dashed) and predicted (solid) rainfall rates for 1-18 September 1974, using Kuo (1965) cumulus parameterization scheme (Krishnamurti et al., 1980).

Anthes (1977) proposed that b could be related to the mean relative humidity in the column by an expression of the form

$$b = \begin{cases} \left[\frac{(1 - \langle RH \rangle)}{(1 - RH_c)}\right]^n & \langle RH \rangle \geq RH_c \\ 1 & \langle RH \rangle < RH_c \end{cases}, \qquad (30)$$

where RH_c is a critical value of relative humidity and n is a positive exponent of order 1 which may be empirically determined. In semi-prognostic tests of the Anthes (1977) scheme, Kuo and Anthes (1984b) found the best agreement between observed and diagnosed rainfall rates when n is between 2 and 3 and RH_c is between 0.25 and 0.50.

Krishnamurti et al. (1980) partitioned the moisture convergence into horizontal and vertical advection and found that the vertical advection

of mixing ratio coincided extremely well with observed rainfall rates during GATE Phase III; they wrote

$$b = -\frac{1}{gM_t}\int_0^{p_s} \underset{\sim}{v}\cdot\nabla q dp \ . \tag{31}$$

Fig. 12 shows the observed and diagnosed rainfall rates during GATE Phase III using a Kuo scheme with b determined by (31). Fig. 13

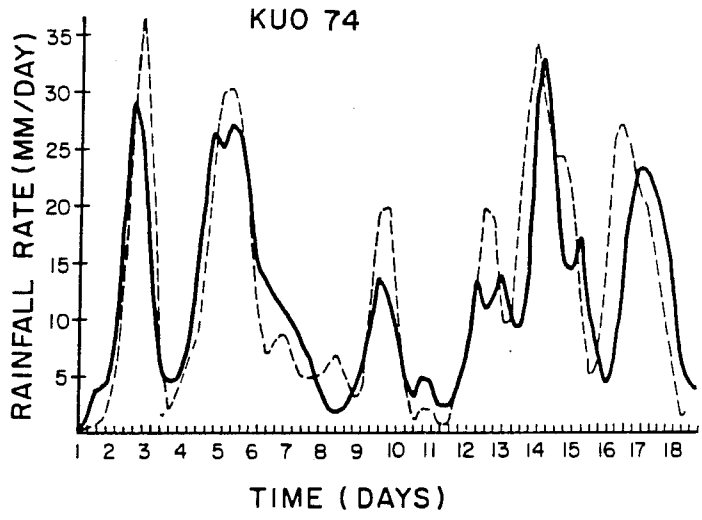

Fig. 12 As in 11, except for Kuo (1974) scheme (Krishnamurti et al., 1980).

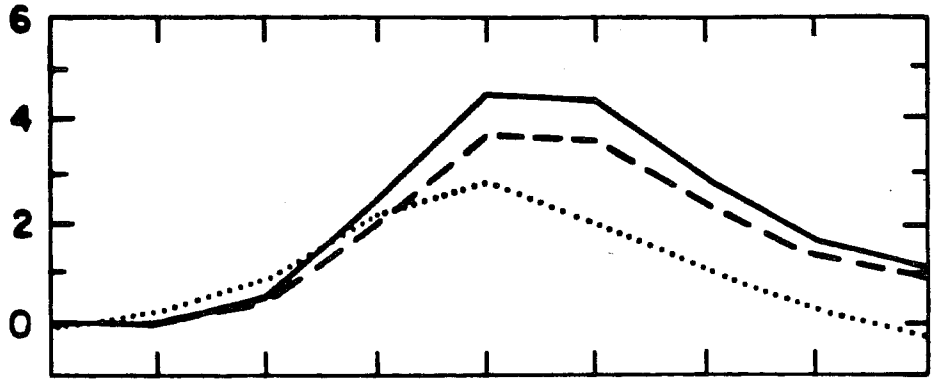

Fig. 13 Observed rainfall rate in cm/day (solid) and that simulated by Krishnamurti et al. (1980, dashed) and Anthes (1977, dotted) over 550 km × 550 km box centered over Oklahoma. The time period (abscissa) begins at 1200 GMT 10 April and ends at 1200 GMT 11 April (Kuo and Anthes, 1984b).

shows the time variation of observed and diagnosed rainfall rates in an extratropical squall system (SESAME-I, 10-11 April 1979) using a Kuo scheme with b given by (30) with n = 1.0 and RH_c = 0.5 and by (31). The success of (31) in diagnosing the observed rainfall rates in a tropical and extratropical system indicates that the net horizontal advection of moisture is not as closely related to precipitation as is the vertical advection, which is reasonable because a strong relationship between upward motion and precipitation is well-known. In contrast, horizontal advection of water vapor of either sign may occur with little vertical motion or precipitation. Apparently, the horizontal advection of water vapor is more closely related to the storage term (S_{qv} in 11).

Molinari (1982) compared the rate at which the standard subtropical sounding (Jordan, 1958) approached a moist neutral condition when a specified vertical motion and moisture supply was used with various formulations of b. Molinari found that the most realistic time evolution of the sounding occurred when a formulation of b was used that required the environmental temperature and mixing ratio to approach the cloud values at the same rate,

$$b = \frac{I + J}{I} \left[\frac{\langle q_c - q \rangle}{\langle q_c - q \rangle + \frac{c_p}{L} \langle T_c - T \rangle} \right] , \tag{32}$$

where J is the net adiabatic temperature change in the column

$$J \equiv - \frac{1}{g} \int_{p_t}^{p_b} \frac{c_p}{L} \frac{T}{\theta} \omega \frac{\partial \theta}{\partial p} \, dp \, . \tag{33}$$

In Molinari's tests, at the initial time $J \approx -0.8I$, so that the b parameter computed from (32) was about 0.2 times the effective b parameter of the original Kuo scheme. This reduction produced a value of b (0.13) much closer to observed values.

3.5 Summary

This paper has reviewed two simple but popular schemes for cumulus parameterization. Two types of convective adjustment have been tested in models and compared to observations. In hard convective adjustment schemes, the model sounding is adjusted so that moist static energy is constant with height. This scheme produces an unrealistic large-scale thermodynamic state and excessive rainfall rates. Better results are obtained with soft adjustment schemes in which small adjustments toward a moist adiabat are made.

Several cumulus parameterization schemes based on Kuo's (1965) original scheme have been used in many numerical models with some success. The relationship of total heating to moisture convergence is a key property of Kuo schemes. A variety of methods of computing the vertical distribution of convective heating and moistening and of computing the parameter b, the fraction of moisture convergence that is assigned to increasing the relative humidity of the column, is discussed. Some of the variations of Kuo-type schemes compared against observations in semi-prognostic tests show considerable accuracy, providing some support for using this type of parameterization in numerical models.

4. REFERENCES

Anthes, R. A., 1977: A cumulus parameterization scheme utilizing a one-dimensional cloud model. Mon. Wea. Rev., 105, 270-286.

Anthes, R. A., 1985: An observational basis for cumulus parameterization. Report of the seminar on progress in numerical modelling and the understanding of predictability as a result of the global weather experiment, Sigtuna, Sweden, October 1984. GARP Special Report No. 43, WMO/TO No. 33. (Available from WMO Case Postale No. 5, CH-1211 Geneva 20, Switzerland), pp. II-1 - II-24.

Anthes, R. A., Y.-H. Kuo, S. G. Benjamin, and Y.-F. Li, 1982: The evolution of the mesoscale environment of severe local storms: Preliminary modeling results. Mon. Wea. Rev., 110, 1187-1213.

Arakawa, A., and W. H. Schubert, 1974: Interaction of a cumulus cloud ensemble with the large-scale environment. Part I. J. Atmos. Sci., 31, 674-701.

Cho, H. R., 1976: Effects of cumulus cloud activity on the large-scale moisture distribution as observed on Reed-Recker's composite easterly waves. J. Atmos. Sci., 33, 1117-1119.

Frank, W. M., 1983: The cumulus parameterization problem. Mon. Wea. Rev., 111, 1859-1871.

Fritsch, J. M., C. F. Chappell, and L. R. Hoxit, 1976: The use of large-scale budgets for convective parameterization. Mon. Wea. Rev., 104, 1408-1418.

Fritsch, J. M., and C. F. Chappell, 1980: Numerical prediction of convectively driven mesoscale pressure systems. Part I: Convective parameterization. J. Atmos. Sci., 37, 1722-1733.

Jordan, C. L., 1958: Mean soundings for the West Indies area. J. Meteor., 15, 91-97.

Kreitzberg, C. W., and D. J. Perkey, 1976: Release of potential instability: Part I. A sequential plume model within a hydrostatic primitive equation model. J. Atmos. Sci., 33, 456-475.

Krishnamurti, T. N., and W. J. Moxim, 1971: On parameterization of convective and nonconvective latent heat release. J. Appl. Meteor., 10, 3-13.

Krishnamurti, T. N., S.-L. Nam, and R. Pasch, 1983: Cumulus parameterization and rainfall rates II. Mon. Wea. Rev., 111, 815-828.

Krishnamurti, T. N., M. Kanamitsu, R. Godbole, C. B. Chang, F. Carr, and J. Chow, 1976: Study of a monsoon depression (II). Dynamical structure. J. Meteor. Soc. Japan, 54, 208-225.

Krishnamurti, T. N., Y. Ramanathan, H.-L. Pan, R. J. Pasch, and J. Molinari, 1980: Cumulus parameterization and rainfall rates I. Mon. Wea. Rev., 108, 465-472.

Kuo, H. L., 1965: On formation and intensification of tropical cyclones through latent heat release by cumulus convection. J. Atmos. Sci., 22, 40-63.

Kuo, H. L., 1974: Further studies of the parameterization of the influence of cumulus convection on large-scale flow. J. Atmos. Sci., 31, 1232-1240.

Kuo, Y.-H., and R. A. Anthes, 1984a: Mesoscale budgets of heat and moisture in a convective system over the central United States. Mon. Wea. Rev., 112, 1482-1497.

Kuo, Y.-H., and R. A. Anthes, 1984b: Semi-prognostic tests of Kuo-type cumulus parameterization schemes in an extratropical convective system. Mon. Wea. Rev., 112, 1498-1509.

Kurihara, Y., 1973: A scheme of moist convective adjustment. Mon. Wea. Rev., 101, 547-553.

Lian, W.-J., 1979: Generalization of Kuo's parameterization of cumulus convection. Papers Meteor. Res., 2, 101-115.

Manabe, S., J. Smagorinsky, and R. F. Strickler, 1965: Simulated climatology of a general circulation model with a hydrological cycle. Mon. Wea. Rev., 93, 769-798.

Miyakoda, K., J. Smagorinsky, R. F. Strickler, and G. D. Hembree, 1969: Experimental extended predictions with a nine-level hemispheric model. Mon. Wea. Rev., 97, 1-76.

Molinari, J., 1982: A method for calculating the effects of deep cumulus convection in numerical models. Mon. Wea. Rev., 11, 1527-1534.